AIP | Applied Physics Letters

Dipole spring ferroelectrics in superlattice SrTiO3/BaTiO3 thin films exhibiting constricted hysteresis loops

Pingping Wu, Xingqiao Ma, Yulan Li, Venkatraman Gopalan, and Long-Qing Chen

Citation: Appl. Phys. Lett. **100**, 092905 (2012); doi: 10.1063/1.3691172
View online: http://dx.doi.org/10.1063/1.3691172
View Table of Contents: http://apl.aip.org/resource/1/APPLAB/v100/i9
Published by the American Institute of Physics.

Dipole spring ferroelectrics in superlattice $SrTiO_3/BaTiO_3$ thin films exhibiting constricted hysteresis loops

Pingping Wu,[1,2,a)] Xingqiao Ma,[1] Yulan Li,[3] Venkatraman Gopalan,[2] and Long-Qing Chen[2]
[1]*Department of Physics, University of Science and Technology Beijing, Beijing 100083, China*
[2]*Department of Materials Science and Engineering, The Pennsylvania State University, University Park, Pennsylvania 16802, USA*
[3]*Pacific Northwest National Laboratory, Richland, Washington 99352, USA*

(Received 8 August 2011; accepted 11 February 2012; published online 1 March 2012)

Ferroelectric superlattice heterostructures have recently been explored for potential applications in electronic devices. In this letter, we employed the phase-field approach to simulate the domain structure and switching of a $(BaTiO_3)_8/(SrTiO_3)_3$ superlattice film constrained by a $GdScO_3$ substrate. A constricted ferroelectric hysteresis loop was observed with a high saturation polarization but a small coercive field. The shape of the hysteresis loop is understood by analyzing the ferroelectric polarization distributions during switching. It is demonstrated that the multilayers stack behaves as dipole spring ferroelectric, named in analogy to exchange spring magnets in magnetic multilayers that show similar loops. © *2012 American Institute of Physics*. [http://dx.doi.org/10.1063/1.3691172]

The development of oxide MBE method[1,2] has enabled the design and growth of superlattice ferroelectric thin films with atomic precision. Among all the multicomponent epitaxial oxide superlattice thin films, the $BaTiO_3$ (BT)/$SrTiO_3$ (ST) superlattice has attracted the most attention due to its chemical stability and adaptive high dielectric constant.[3–10] However, although numerous experimental and theoretical works[9–14] have been reported on the transition temperature (T_c), the polarization distribution, and the phase structure of ferroelectric thin films, the polarization switching of superlattice films by an external electric field is one of the least studied. Different from the corresponding regular composite, the ferroelectric superlattice is very sensitive to substrate and the stacking configuration.[3–10,15,16]

In this letter, we report an interesting constricted hysteresis loop in the superlattice structure BT_8/ST_3 obtained using phase-field simulations and investigate the corresponding domain structure and polarization distribution of the superlattice under an electric field. We describe the ferroelectric domain evolution of a ferroelectric superlattice, i.e., the polarization distribution, using the time-dependent Ginzburg-Landau (TDGL) equations,

$$\frac{\partial P_i(x,t)}{\partial t} = -L\frac{\delta F}{\delta P_i(x,t)}, \quad (i = 1,2,3), \tag{1}$$

where P_i is the ferroelectric polarization component, $x_i = (x_1, x_2, x_3)$ is the coordinate, t is time, L is the kinetic coefficient, and F is the total energy of the BT/ST superlattice system. The total energy is expressed by

$$F = F_{bulk}(P_i) + F_{grad}(\partial P_i/\partial x_j) + F_{elast}(P_i, \varepsilon_{ij}) + F_{elec}(P_i, E_i), \tag{2}$$

in which F_{bulk} is the bulk chemical energy, for a centrosymmetric crystal, which can be expended in the form

$$F_{bulk}(P_i) = \int_v \left[\frac{1}{2}\alpha_{ij}P_iP_j + \frac{1}{4}\gamma_{ijkl}P_iP_jP_kP_l + \frac{1}{6}\omega_{ijklmn}P_iP_jP_kP_lP_mP_n\right]d^3x, \tag{3}$$

where α_{ij}, γ_{ijkl}, and ω_{ijklmn} are the phenomenological Landau expression coefficients under zero external stress and external electric field.

F_{grad} in Eq. (2) is the gradient energy, which is introduced through the gradients of the polarization field, i.e.,

$$F_{grad}(\partial P_i/\partial x_j) = \int_v \left[\frac{1}{2}G_{ijkl}\frac{\partial P_i}{\partial x_j}\cdot\frac{\partial P_k}{\partial x_l}\right]d^3x, \tag{4}$$

where G_{ijkl} is the gradient energy coefficients.

Based on Khachaturyan's elastic theory,[17] the elastic energy term F_{elast} is given by

$$F_{elast}(P_i, \varepsilon_{ij}) = \int_v \left[\frac{1}{2}c_{ijkl}(\varepsilon_{ij} - Q_{ijkl}P_kP_l)(\varepsilon_{kl} - Q_{klij}P_iP_j)\right]d^3x, \tag{5}$$

where ϵ_{ij} is the strain component. c_{ijkl} is the elastic stiffness tensor, and Q_{ijkl} represents the electrostrictive coefficients.

F_{elec} can be written as

$$F_{elec}(P_i, E_i) = -\int_v \left(\frac{1}{2}k_b\varepsilon_o E_i^2 + E_iP_i\right)d^3x, \tag{6}$$

where E_i is total electric field and ε_o is the vacuum permittivity. The use of a background dielectric constant, k_b, rather than 1 was discussed in Refs. 18–21.

In the simulation, we discretized the simulation cell using $(64\Delta x_1 \times 64\Delta x_2) \times N\Delta x_3$, where $\Delta x_1 = \Delta x_2 = 1$ nm, $\Delta x_3 = 0.5a_{sub}$ ($GdScO_3$) $\approx$ 0.2 nm, and $N = 2(m+n)$ for a BT_m/ST_n superlattice structure. Periodical boundary conditions are employed along the x_1, x_2, and x_3 directions. The

a)Author to whom correspondence should be addressed. Electronic mail: pingpingwu-ustb@126.com.

Devonshire's bulk free energy coefficients, the electrostrctive and the elastic coefficients given in Refs. 11 and 12 are employed here: for BT layers, $\alpha_1 = 4.124(T - 388) \times 10^5$, $\alpha_{11} = -2.097 \times 10^8$, $\alpha_{12} = 7.974 \times 10^8$, $\alpha_{111} = 1.294 \times 10^9$, $\alpha_{112} = -1.950 \times 10^9$, $\alpha_{123} = -2.500 \times 10^9$, $\alpha_{1111} = 3.863 \times 10^{10}$, $\alpha_{1112} = 2.529 \times 10^{10}$, $\alpha_{1122} = 1.637 \times 10^{10}$, $\alpha_{1123} = 1.367 \times 10^{10}$, $c_{11} = 1.78 \times 10^{11}$, $c_{12} = 0.964 \times 10^{11}$, $c_{44} = 1.22 \times 10^{11}$, $Q_{11} = 0.10$, $Q_{12} = -0.034$, $Q_{44} = 0.029$, and for ST layers: $\alpha_1 = 2.6353[\coth(42/T) - 0.90476] \times 10^7$, $\alpha_{11} = 1.696 \times 10^9$, $\alpha_{12} = 1.373 \times 10^9$, $c_{11} = 3.36 \times 10^{11}$, $c_{12} = 1.07 \times 10^{11}$, $c_{44} = 1.27 \times 10^{11}$, $Q_{11} = 0.066$, $Q_{12} = -0.0135$, and $Q_{44} = 0.0096$, where c_{ij} and Q_{ij} are the Voigt notation for c_{ijkl} and Q_{ijkl} in SI units and T in Kelvin. The pseudocubic lattice parameter for the BT and ST layers are set to be $a_{BT} = 3.9994 \times 10^{-10} + 5.35386 \times 10^{-15}$ $(T - 273)$, and $a_{ST} = 3.9043 \times 10^{-10}[(1 + 9.39) \times 10^{-6}$ $(T - 273) + 1.97 \times 10^{-9}$ $(T - 273)^2]$, where T is in Kelvin.

Figures 1(a) and 1(b) shows a stable simulated domain structure of a superlattice BT_8/ST_3 at room temperature obtaining using the vacuum permittivity. The superlattice is constrained on the substrate of $GdScO_3$. The in-plane lattice parameter of the substrate $GdScO_3$ at room temperature ($\sim$3.968 Å) is close to the average lattice parameter of the whole superlattice heterostructure, i.e., $a_{ave\text{-}sup}(BT_8/ST_3) = (8a_{BT} + 3a_{ST})/11 = 3.975$ Å. As a result of the substrate contribution, the ST layers of the superlattice are under a biaxial tensile strain of 1.6% while the BT layers are under a compressive strain of −0.85%. According to our previously calculated phase diagram,[22,23] the BT layers contain tetragonal *c* domains (Figure 1(a)), and the ST layers remained in the orthorhombic phase. Due to the superlattice stacking configuration of BT_8/ST_3 and the electrostatic interaction between the polarizations of BT layers and ST layers, however, we observed the mixed orthorhombic/monoclinic phases in the ST layers (Figure 1(b)).

The polarization distribution could also be illustrated by the cross-section polarization vector map of Figure 1(c). In the BT layers, the polarization is orientated along the [001] or $[00\bar{1}]$ direction, while in the ST layers, some polarization rotates due to the electronic dipole-dipole interaction, and thus, mixed orthorhombic/monoclinic phases generated. It should be noticed that the polarization vector map exhibits an enhanced mixed Bloch-Néel-Ising wall with the alternating handedness polarization vortices in traversing the domain wall normal.[24] The vector map proves that the heterostructure resulted from a balance of the gradient energy and electrostatic energy under the in-plane substrate induced strain.

The polarization-electric field hysteresis loop (PE loop) of the superlattice BT_8/ST_3 on the $GdScO_3$ substrate is presented in Figure 2 with the applied electric field in the thickness direction. It clearly demonstrates an interesting constricted ferroelectric hysteresis loop (also known as "broken loops" in Ref. 25). Usually, the constricted loop occurs when internal defects or fields randomly distribute or in the aging process for the ceramics. The constricted loop was also obtained in the theoretical and experimental study of perovskite lead zirconate titanate (PZT) systems.[26–28] For a comparison, simulations with several different values of background dielectric constant were chosen to investigate its influence on the hysteresis loops. The red, blue, green, and dark green lines represents $k_b = 1$, 5, 10, and 50, respectively. It clearly shows that $k_b = 1$ and 5 produce very similar constricted loops but not for $k_b = 50$, while $k_b = 10$ case is somewhere in-between. Therefore, the predicted constricted loops may not be observed if there is presence of space charges in the experimental samples, and they can respond under an applied electric field, i.e., if they are not frozen.

In order to understand the constricted loop of the BT/ST superlattice heterostructure, the evolution of the polarization

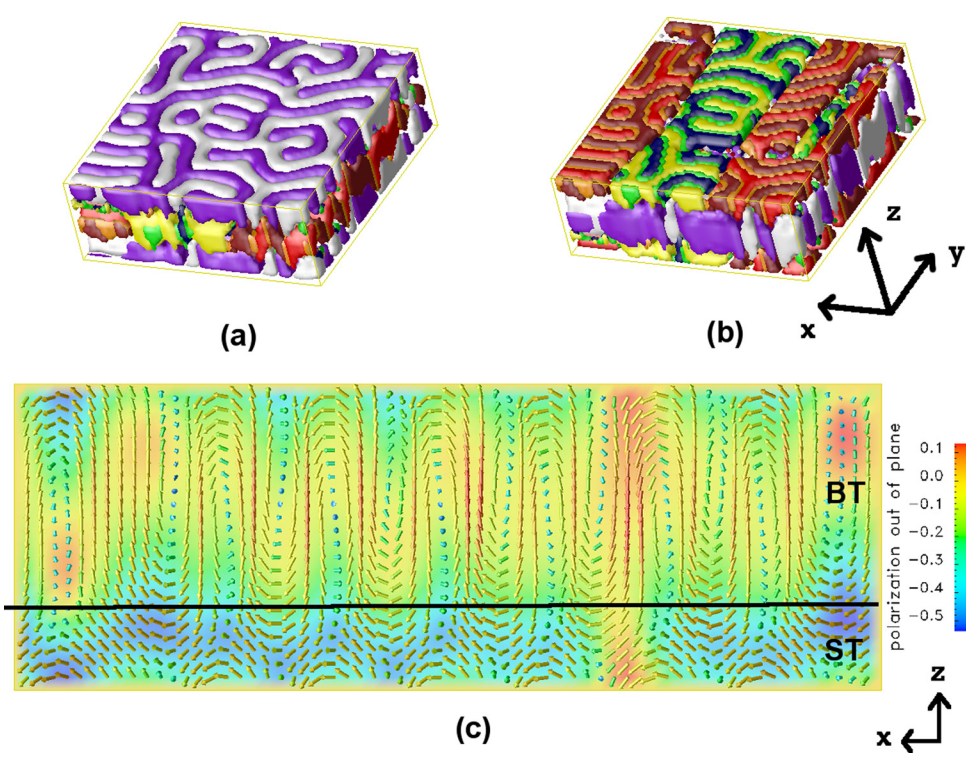

FIG. 1. (Color online) The ferroelectric domain structure in a superlattice of BT_8/ST_3 shown with the BT layer on top surface (a), and the ST layer on the surface (b), respectively. The white and purple colors in the BT layer indicate the tetragonal c+ and c− domains, respectively. The mixed monoclinic (represented by blue, yellow, red, and dark red)/orthorhombic (represented by orange and green) phases are observed in the ST layer. (c) The polarization vector map at one cross-section plane of the domain structure in (a) or (b); the value of the polarization out of plane (see color bar) are reduced by $P_0 = 0.26\,C/m^2$.

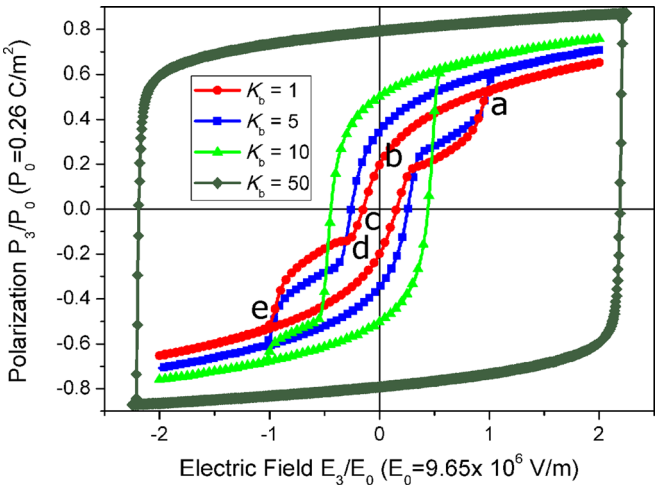

FIG. 2. (Color online) The constricted PE hysteresis loop of BT_8/ST_3 superlattice on $GdScO_3$ substrate, at room temperature. Several different values of background dielectric constant are used to investigate the influence of background dielectric constant on the hysteresis loop. The circle, square, triangle, diamond symbol lines represents $k_b = 1$, 5, 10, and 50, respectively.

distribution during the switching process was shown in Figure 3. Figures 3(a)–3(e) display the polarization vector maps at the points a-e of the hysteresis loop of Figure 2 ($k_b = 1$). The arrow and the color of Figure 3 represent the direction and the magnitude of a polarization, respectively. Figure 3(a) shows the initial switching process where we see slight rotations of the polarizations in both the BT layers and ST layers. As a result of the tensile in-plane strain imposed in the ST layers, the rotation angles of the polarizations in ST layers are generally larger than those in the BT layers. When the external electric field decreased to zero, i.e., at point b in Figure 2, the magnitude of the polarizations at the center of the BT layers decreased, and the polarizations in the ST layers and at the interface between the BT and ST layers rotated toward to the x_1-x_2 plane. In the following stage, as the electric field increased in the opposite direction, the polarizations formed vortex structures as shown in Figure 3(c), which shows a similar structure as Figure 1(c). The overall polarization of the whole system at point *c* is zero. Thus, further increasing the external electric field in the opposite direction will favor the tetragonal "–*c*" domain in the BT layers and gives a negative total polarization. The corresponding polarization distribution is shown in Figure 3(d). It can be seen that more domain walls appear in the superlattice domain structure, in order to decrease the electric static energy. In this process, we see a significant increase of the absolute magnitude of the total polarization, reflected in the PE loop of Figure 2. When the external field increased further, only a slight increase of the polarization absolute magnitude is observed due to the domain wall movement. Finally, as all the polarizations switched to along the –z direction, we see the completion of a constricted loop of the BT/ST superlattice.

From the simulations, we observed that the formation of a constricted hysteresis loop and the corresponding polarization distribution evolution. It raises the possibility that the shape of the PE loop can be designed by growing specific ST/BT superlattice configurations on different substrates with the knowledge, in which the PE hysteresis loop of BT

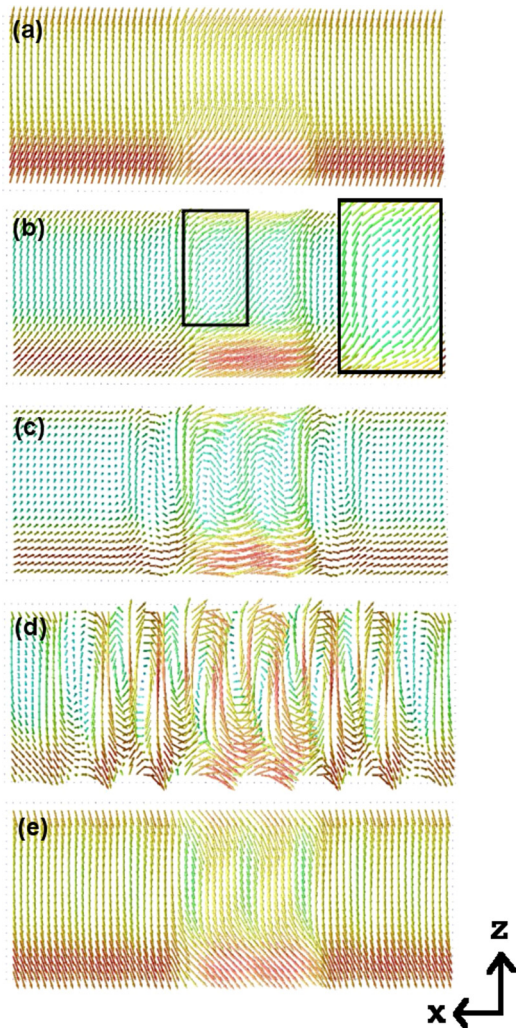

FIG. 3. (Color online) The polarization distribution vector maps (a)-(e) are corresponding to the points a-e in Figure 2, respectively.

single crystal has high coercive field and high remnant polarization,[29,30] while ST single crystal is paraelectric phase at room temperature. Also, we note that the constricted loop is similar to the magnetic hysteresis of exchange-coupled systems (also known as *exchange-spring magnets*),[31] which are magnetic multilayer nanostructures combined large saturation magnetization of soft magnets with the high anisotropy of hard magnets, designed for its applications on ultra-high density magnetic storage and sensors. Due to the similarity between the superlattice PE loop and the hysteresis of exchange-spring magnets, we name the multilayers as *dipole spring ferroelectrics*, referring to the dipole-dipole interactions that give rise to the pinched loops and reversible behavior, and could show significant potential for applications to ferroelectric memory and capacitor devices. The loop section *a-b* is completely reversible without hysteresis, in going back and forth along the field axis. In principle, the complete section of *a-d* could be designed to be reversible without hysteresis (similar to exchange spring magnets), if the domain pinning due to the $SrTiO_3$ was stronger.

In summary, we investigated the domain structure and the switching process of the superlattice BT_8/ST_3 on the $GdScO_3$ substrate based on the phase-field approach. We report a constricted P-E hysteresis loop in our simulation

that shows a relative high remnant polarization but a small coercive field, with large loop sections of reversibility without hysteresis. The evolution of the polarization distributions is analyzed during the switching process to understand the constricted loop. It is shown that the constricted PE loop is similar to the hysteresis in magnetic exchange-spring systems, which raises the potential application of designing novel *dipole spring ferroelectrics* for electronic memory technology and capacitor devices.

This work was supported by the NSF under the Grant Nos. DMR-1006541, NSF-DMR-0908718, and partially by NSF-DMR-0820404. The computer simulations were carried out on the LION and Cyberstar clusters at the Pennsylvania State University supported in part by NSF Major Research Instrumentation Program through Grant No. OCI-0821527 and in part by the Materials Simulation Center and the Graduated Education and Research Services at the Pennsylvania State University.

[1]D. G. Schlom, L. Q. Chen, C. B. Eom, K. M. Rabe, S. K. Streiffer, and J. M. Triscone, Annu. Rev. Mater. Sci. **37**, 589 (2007).
[2]D. G. Schlom, L. Q. Chen, X. Q. Pan, A. Schmehl, and M. A. Zurbuchen, J. Am. Ceram. Soc. **91**, 2429 (2008).
[3]H. Tabata, H. Tanaka, and T. Kawai, Appl. Phys. Lett. **65**, 1970 (1994).
[4]T. Shimuta, O. Nakagawara, T. Makino, S. Arai, H. Tabata, and T. Kawai, J. Appl. Phys. **91**, 2290 (2002).
[5]J. Kim, Y. Kim, Y. S. Kim, J. Lee, L. Kim, and D. Jung, Appl. Phys. Lett. **80**, 3581 (2002).
[6]J. B. Neaton and K. M. Rabe, Appl. Phys. Lett. **82**, 1586 (2003).
[7]S. Rios, A. Ruediger, A. Q. Jiang, J. F. Scott, H. Lu, and Z. Chen, J. Phys.: Condens. Matter. **15**, L305 (2003).
[8]K. Johnston, X. Y. Huang, J. B. Neaton, and K. M. Rabe, Phys. Rev. B **71**, 100103(R) (2005).
[9]S. Lisenkov and L. Bellaiche, Phys. Rev. B **76**, 020102(R) (2007).
[10]D. A. Tenne, A. Bruchhausen, N. D. Lanzillotti-Kimura, A. Fainstein, R. S. Katiyar, A. Cantarero, A. Soukiassian, V. Vaithyanathan, J. H. Haeni, W. Tian *et al.*, Science **313**, 1614 (2006).
[11]Y. L. Li, S. Y. Hu, D. Tenne, A. Soukiassian, D. G. Schlom, X. X. Xi, K. J. Choi, C. B. Eom, A. Saxena, T. Lookman *et al.*, Appl. Phys. Lett. **91**, 112914 (2007).
[12]Y. L. Li, S. Y. Hu, D. Tenne, A. Soukiassian, D. G. Schlom, L. Q. Chen, X. X. Xi, K. J. Choi, C. B. Eom, A. Saxena *et al.*, Appl. Phys. Lett. **91**, 252904 (2007).
[13]J. H. Lee, J. Yu, and U. V. Waghmare, J. Appl. Phys. **105**, 016104 (2009).
[14]T. Harigai, D. Tanaka, H. Kakemoto, S. Wada, and T. Tsurumi, J. Appl. Phys. **94**, 7923 (2003).
[15]M. Dawber, N. Stucki, C. Lichtensteiger, S. Gariglio, P. Ghosez, and J. M. Triscone, Adv. Mater. **19**, 4153 (2007).
[16]E. Bousquet, M. Dawber, N. Stucki, C. Lichtensteiger, P. Hermet, S. Gariglio, J. M. Triscone, and P. Ghosez, Nature (London) **452**, 732 (2008).
[17]A. G. Khachaturyan, *Theory of Structural Transformations in Solid* (Wiley, New York, 1983).
[18]A. K. Tagantsev, Ferroelectrics **69**, 321 (1986).
[19]A. K. Tagantsev, Ferroelectrics **375**, 19 (2008).
[20]C. H. Woo and Y. Zheng, Appl. Phys. A **91**, 59 (2008).
[21]C. Kittel, *Introduction to Solid State Physics*, 7th ed. (Wiley, New York, 1996).
[22]Y. L. Li, S. Choudhury, J. H. Haeni, M. D. Biegalski, A. Vasudevarao, A. Sharan, H. Z. Ma, J. Levy, V. Gopalan, S. Trolier-McKinstry *et al.*, Phys. Rev. B **73**, 184112 (2006).
[23]Y. L. Li and L. Q. Chen, Appl. Phys. Lett. **88**, 072905 (2006).
[24]D. Lee, R. K. Behera, P. P. Wu, H. X. Xu, Y. L. Li, S. B. Sinnott, S. R. Phillpot, L. Q. Chen, and V. Gopalan, Phys. Rev. B **80**, 060102(R) (2009).
[25]D. Damjanovic, Rep. Prog. Phys. **61**, 1267 (1998).
[26]A. N. Morozovska and E. A. Eliseev, J. Phys.: Condens. Matter **16**, 8937 (2004).
[27]Q. Y. Jiang, E. C. Subbarao, and L. E. Cross, J. Appl. Phys. **75**, 7433 (1994).
[28]T. Tamura, K. Matsuura, H. Ashida, K. Kondo, and S. Otani, Appl. Phys. Lett. **74**, 3395 (1999).
[29]S. Choudhury, Y. L. Li, L. Q. Chen, and Q. X. Jia, Appl. Phys. Lett. **92**, 142907 (2008).
[30]J. Y. Jo, Y. S. Kim, T. W. Noh, J. G. Yoon, and T. K. Song, Appl. Phys. Lett. **89**, 232909 (2006).
[31]E. F. Kneller and R. Hawig, IEEE. Trans. Magn. **27**, 3588 (1991).